However, at high bias the modulation mostly affects carrier population on excited states, which have shorter carrier lifetime due to both increased nonradiative recombination and an alternative relaxation channel to lower states [7]. This shorter carrier lifetime, also observed independently by time-resolved photoluminescence measurements, results in the observed increase of the modulation bandwidth with bias.

The same setup was used to investigate 35 and 186 μm size devices. At a bias of 20 mA, the 186 μm devices showed a maximum bandwidth of about 400 MHz, while for the 35 μm devices we found a maximum bandwidth of above 1 GHz at 8 mA of the driving current.

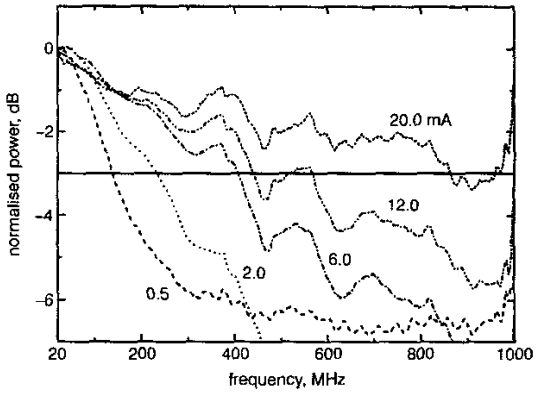

Fig. 2 *Normalised modulation response curves for 84 μm device at different driving currents*

Data transmission experiments: For digital modulation, the scalar network analyser is replaced by a pulse pattern generator on the transmission side. In the detection circuit the same PD was used. After two amplifiers, totaling about 50 dB of gain, the bit pattern was viewed on a digital sampling oscilloscope.

We use the 84 μm device described previously at a bias of 12 mA. The generator is set for a modulation voltage of 1.6 V_{pp} out of its 50 Ω impedance port. Using a repetitive 1-0-bit sequence at a data rate of 1Gbit/s we recorded the wide open and symmetric eye diagram shown in Fig. 3*a*. With a pseudo-random bit sequence of $2^7 - 1$ word length at 300 Mbit/s we could detect the open, but somewhat asymmetric eye diagram seen in Fig. 3*b*. Again we use the 84 μm device biased at 12 mA of DC current. The modulator output was set for 2 V_{pp}.

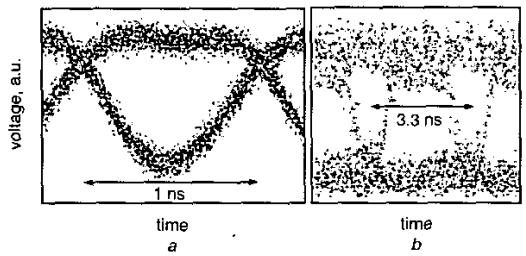

Fig. 3 *Eye diagram for alternating 1-0-bit sequence transmitted at 1 Gbit/s and PRBS signal at 300 Mbit/s both using 84 μm LED*
a Alternating bit sequence *b* PRBS signal

Conclusions: In conclusion, we have demonstrated up to 1 Gbit/s data transmission employing single-mirror vertically emitting LEDs operating around 1.3 μm wavelength from self-assembled InAs-InGaAs quantum dots on GaAs substrate. This shows that QD LEDs may be suitable as low-cost sources for short-distance 1.3 μm optical links.

Acknowledgments: The authors would like to acknowledge support by the European Community under IST Project 'GSQ'.

15 May 2002
Electronics Letters Online No: 20020646
DOI: 10.1049/el:20020646

M. Kicherer, R. Michalzik (*Department of Optoelectronics, University of Ulm, D-89069 Ulm, Germany*)

E-mail: max.kicherer@e-technik.uni-ulm.de

A. Fiore, U. Oesterle, R.P. Stanley, M. Ilegems (*Institute for Micro-Optoelectronics, Ecole Polytechnique Fèdèrale de Lausanne, CH-1015 Lausanne, Switzerland*)

References

1 PARK, G., SHCHEKIN, O.B., HUFFAKER, D.L., and DEPPE, D.G.: 'Low-threshold oxide-confined 1.3-μm quantum-dot laser', *IEEE Photonics Technol. Lett.*, 2000, **12**, (3), pp. 230–232

2 SHERNYAKOV, Y.M., BEDAREV, D.A., KONDRATEVA, E.Y., KOPEV, P.S., KOVSH, A.R., MALEEV, N.A., MAXIMOV, M.V., MIKHRIN, S.S., TSATSULNIKOV, A.F., USTINOV, V.M., VOLOVIK, B.V., ZHUKOV, A.E., ALFEROV, Z.I., LEDENTSOV, N.N., and BIMBERG, D.: '1.3 μm GaAs-based laser using quantum dots obtained by activated spinoidal decomposition', *Electron. Lett.*, 1999, **35**, (11), pp. 898–900

3 MUKAI, K., NAKATA, Y., OTSUBO, K., SUGAWARA, M., YOKOYAMA, N., and ISHIKAWA, H.: '1.3 μm CW lasing of InGaAs-GaAs quantum dots at room temperature with a threshold current of 8 mA', *IEEE Photonics Technol. Lett.*, 1999, **11**, (10), pp. 1205–1207

4 HUANG, X., STINTZ, A., HAINSA, C.P., LIU, G.T., CHENG, J., and MALLOY, K.J.: 'Efficient high-temperature CW lasing operation of oxide-confined long-wavelength InAs quantum dot lasers', *Electron. Lett.*, 2000, **36**, (1), pp. 41–42

5 FIORE, A., OESTERLE, U., STANLEY, R.P., and ILEGEMS, M.: 'High-efficiency light-emitting diodes at ≈1.3 μm using InAs-InGaAs quantum dots', *IEEE Photonics Technol. Lett.*, 2000, **12**, (12), pp. 1601–1603

6 DEPPE, D.G., CAMPBELL, J.C., KUCHIBHOLTA, R., ROGERS, T.J., and STREETMAN, B.G.: 'Optically-coupled mirror-quantum well InGaAs-GaAs light emitting diode', *Electron. Lett.*, 1990, **26**, (20), pp. 1665–1666

7 GRUNDMANN, M., and BIMBERG, D.: 'Theory of random population for quantum dots', *Phys. Rev. B*, 1997, **55**, (15), pp. 9740–9745

Modulation transfer function and quantum efficiency in thin semiconductor photodetectors

D. Abbott

For the first time, the correct equation for quantum efficiency, and hence modulation transfer function (MTF) in a semiconductor of finite thickness, is reported. This first-order analysis considers only the three basic effects of absorption coefficient, minority carrier diffusion length and depletion width. This is of interest in the first-order design of photodetectors, optical smart sensors and solid-state imagers.

Introduction: Quantum efficiency is the measure of the number of electrons per incident photon that are collected in a photodetector. For conventional semiconductor photodetectors the quantum efficiency η is always a number less than unity. The correct formula for quantum efficiency for a frontside illuminated photodetector on a bulk substrate is given by

$$\eta_{\text{bulk}} = T(\lambda)\left(1 - \frac{e^{-\alpha W}}{1 + \alpha L_o}\right) \quad (1)$$

where T is the transmission coefficient of light through the passivation layers, W is the depletion width, α is the optical absorption coefficient and L_o is the minority carrier diffusion length in the semiconductor. This equation was first derived in 1974 by Seib [1]. Seib's formula approximates to the case of a bulk semiconductor as he assumed the boundary conditions for a semi-infinite slab of material.

However, nowadays, for many practical cases this assumption is no longer valid, owing to the prevalence of epitaxial substrates. This requires us to compute the quantum efficiency in a thin slab of material, rather than a semi-infinite slab. Correct analysis of the thin-slab case is of importance for optical smart sensors, imaging arrays, multiple quantum well devices, etc., that are now being used for applications such as in imaging, spatial light modulators, optoelectronic circuits, etc. In the open literature, to our knowledge, there is no correct analysis presented for the thin-slab case.

As a first step, in this Letter we present the first-order case where only the depletion width W, absorption coefficient α and the minority carrier diffusion length L_o are taken into account.

Quantum efficiency analysis in a thin slab: The governing equation for the penetration of light into a material is given by Lambert's law of absorption (also known as Bouguer's or Beer's law),

$$\Phi(x) = \Phi_o e^{-\alpha x}$$

where Φ is the incident photon flux per unit area. Consider a slab of semiconductor material, with finite thickness, h. For mathematical convenience, let the surface be at $x = -W$, the depletion region edge be at $x = 0$ and the backside be at $x = h - W$. The continuity equation balance for generation and recombination under steady-state is:

$$-D\nabla^2 n + \frac{n}{\tau} = G \tag{2}$$

where D is the diffusion constant, n is the minority carrier concentration in the undepleted region, τ is minority carrier lifetime and G the electron-hole pair generation rate. We shall use n to denote either n- or p-type carriers as this analysis is independent of whether electrons or holes are the minority carriers, so long as the correct coefficient values for holes or electrons are used in any particular instance. The generation rate G is given by

$$G = \Phi\alpha e^{-\alpha x} \tag{3}$$

Combining the above equations with the expression for minority carrier diffusion length, $L_o = \sqrt{(D\tau)}$, we can rewrite the continuity equation as

$$\frac{d^2 n}{dx^2} - \frac{n}{L_o^2} = -\frac{1}{D}\Phi\alpha e^{-\alpha(x+W)} \tag{4}$$

We solve, asserting boundary conditions at the depletion edge $x = 0$, $n = 0$ and at the slab backside $x = h - W$, $n = 0$ and can then find the steady-state carrier flux which is given by

$$J = \int_{-W}^{0} \Phi(1 - e^{-\alpha W}) + D\left.\frac{\partial n}{\partial x}\right|_{x=0} \tag{5}$$

After some manipulation, using $\eta = J/\Phi$, we get

$$\eta = 1 - \frac{e^{-\alpha W}}{1 + \alpha L_o} - \frac{\alpha L_o e^{-\alpha W}}{\alpha^2 L_o^2 - 1}\frac{e^{-h/L_o} - e^{-h\alpha}}{\sinh(h/L_o)} \tag{6}$$

This equation shows that the quantum efficiency equals that of the semi-infinite case *plus* a (negative) second-order term. It is quite remarkable and elegant that these two terms can be separately identified. Both this expression and the realisation that the semi-infinite case *plus* a second-order term yields the finite slab case which seems to appear nowhere in the literature. Note that this expression has all the expected features. Each term is dimensionless, i.e. each argument is a ratio of two lengths or an absorption coefficient times a length. This is an important feature that is missing in some erroneous attempts found in the literature. Also for $h \to \infty$ the expression reduces to the semi-infinite case.

The function is also well-behaved in that quantum efficiency goes down, as expected, for increasing absorption length, Fig. 1, and goes up for increasing diffusion length, Fig. 2. Another important feature is that, by inspection, η always stays below unity; this is illustrated for specific examples in the Figures.

If we let

$$\eta_+ = T(\lambda)\frac{\alpha L_o e^{-\alpha W}}{\alpha^2 L_o^2 - 1}\frac{e^{-h/L_o} - e^{-h\alpha}}{\sinh(h/L_o)}$$

we see the remarkable result that $\eta_{\text{epi}} = \eta_{\text{bulk}} - \eta_+$, where η_+ is the quantum efficiency of the highly-doped substrate beneath the epitaxial layer. Note that this formula assumes that recombination in the highly-doped substrate is instantaneous; this approximation is accurate for most practical cases. The ability to separate η_{epi} into two clearly identifiable terms is significant, as the modulation transfer function (MTF) can then also be separated and the two terms can be analysed separately in a physically meaningful way.

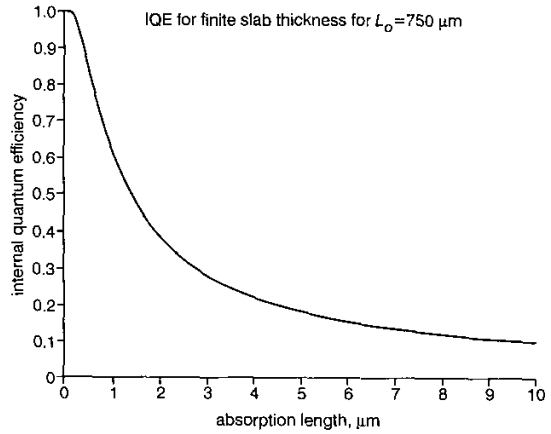

Fig. 1 *Quantum efficiency against absorption length*

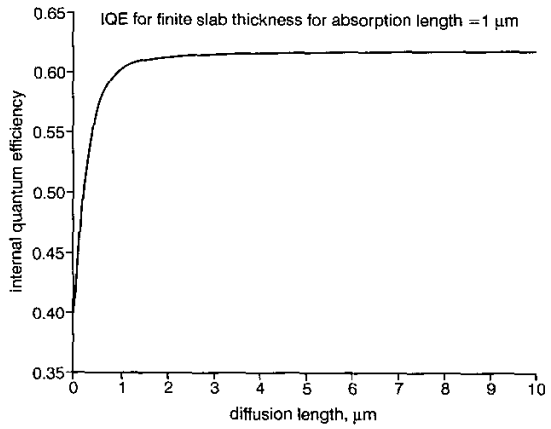

Fig. 2 *Theoretical MTF against spatial frequency*

Discussion: Both (6) and the realisation that it can be separated into two physically identifiable terms has not been reported in the open literature. The quantum efficiency formulae are generally poorly presented in the literature. For instance, a recent attempt at a formula [2] for η_{epi} is dimensionally incorrect, does not have separable terms and under some conditions produces values greater than unity. Note that our expression (6) has all the expected features. Each term is dimensionless, i.e. each argument is a ratio of two lengths or an absorption coefficient times a length. This is an important feature which is missing in other work. Also for $h \to \infty$ our expression reduces to the semi-infinite case. Our function is also well-behaved in that quantum efficiency goes down for increasing absorption length, as expected, and goes up for increasing diffusion length. Another important feature is that, by inspection, (6) always stays below unity.

There is also some confusion in the literature over (1). Our equation agrees with the derivation in the seminal work of Seib [1] and with a fair body of literature. However, there is also a formula due to Barbe [3] that appears in some of the literature, such as in McCaughan and Holeman [4]. Barbe's expression is in terms of MTF and on inspection it can be seen to be clearly too optimistic.

MTF analysis – spatial degradation by diffusion: An ideal MTF has the value of unity and it has the behaviour that if either quantum efficiency or spatial resolution decreases, then MTF also decreases below unity. The definition of MTF is simply [1]

$$\text{MTF} = \frac{\eta_k}{\eta}$$

where η_k is given by the same formula as the quantum efficiency, η, but with each L_o term substituted by $\sqrt{\{(1/L_o^2) + (2\pi k)^2\}}$ and k is the spatial frequency.

This is shown in Fig. 3, where the importance of epi rather than bulk substrates for silicon is demonstrated. Although the diffusion curve for

a wavelength of 550 nm in bulk is acceptable, the MTF for 800 nm is severely degraded in bulk compared to epi.

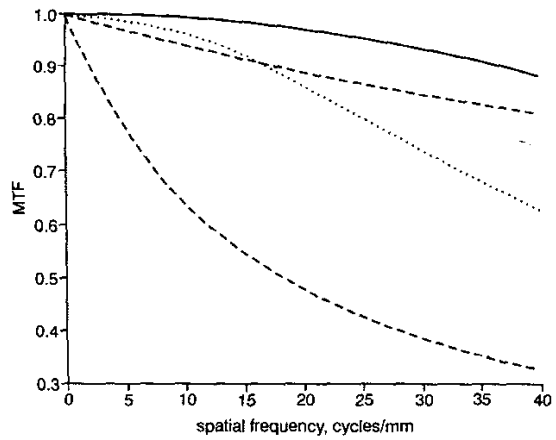

Fig. 3 *Quantum efficiency against diffusion length*
Diffusion-only curves are:
-·- Si bulk, 550 nm
··· Si epi, 800 nm
--- Si bulk, 800 nm
— geometrical-only curve is for 7/20 aperture-to-pitch ratio and is included for reference

The geometrical-only curve is obtained from the usual sinc function expression and represents the ideal case in the absence of diffusion effects.

Conclusion: In the first-order analysis of quantum efficiency, we have disputed the equation for quantum efficiency in a frontside illuminated finite slab given in recent literature. From first principles we derive the correct first-order equation, which has not been previously reported in the open literature. This result is significant as the equation can be separated into two physically meaningful terms. This new perspective will be useful for simplifying MTF analysis in epi substrates. Furthermore, we have disputed the MTF equation in bulk due to Barbe and have highlighted the validity of Seib's bulk equation. An open question is to extend our analysis to include the effect of surface states and other second-order effects.

Acknowledgments: This work was supported by the Australian Research Council and the Sir Ross and Sir Keith Smith Fund (Australia).

6 February 2002
Electronics Letters Online No: 20020546
DOI: 10.1049/el:20020546

D. Abbott (*Centre for Biomedical Engineering (CBME) and Department of Electrical & Electronic Engineering, Adelaide University, SA 5005, Australia*)

E-mail: dabbott@eleceng.adelaide.edu.au

References

1 SEIB, D.H.: 'Carrier diffusion degradation of modulation transfer function in charge coupled imagers', *IEEE Trans. Electron Devices*, 1974, **21**, (3), pp. 210–217
2 THEUWISSEN, A.J.P.: 'Solid-state imaging with charge-coupled devices' (Kluwer, 1995), p. 135
3 BARBE, D.F.: 'Imaging devices using the charge-coupled concept', *Proc. IEEE*, 1975, **63**, pp. 38–67
4 MCCAUGHAN, D.V., and HOLEMAN, B.R.: *in* HOWES, M.J., and MORGAN, D.V. (Eds): 'Charge-coupled devices and systems' (Wiley, 1979), Chap. 5, pp. 241–295

p-type quantum well infrared photodetectors covering wide spectrum

H.C. Liu, T. Oogarah, E. Dupont, Z.R. Wasilewski, M. Byloos, M. Buchanan, F. Szmulowicz, J. Ehret and G.J. Brown

Using a set of *p*-type GaAs/AlGaAs quantum well infrared photodetectors, a wide spectral coverage is demonstrated. Photoresponses at wavelengths as short as 1.4 μm and as long as 15 μm are shown. The shortest wavelength device with a high Al fraction (95%) peaks at 1.9 μm and covers a range of 1.4 to 3 μm.

The *n*-type quantum well infrared photodetector (QWIP) based on GaAs/AlGaAs epitaxial materials is now an established technology [1, 2]. However, *p*-type QWIPs offer some advantageous properties such as normal incidence [3] and broad photoresponse spectrum. We have therefore carried out a systematic set of experiments in optimising a P-QWIP design for covering the 3–5 μm region [4–7]. Device parameters such as well width and barrier height [4], well doping [5], and barrier thickness [6] were varied. In a microcavity P-QWIP, a peak absorption of 25% was achieved [7]. Our experimental work was guided by theory [8, 9].

Based on our study, the optimum design of *p*-type quantum well is such that the HH1 to LH2 transition is utilised with LH2 being in resonance with the top of the barrier. For the GaAs/$Al_xGa_{1-x}As$ system, the valence band offset of $\Delta E_v = 0.53x$ eV best matches with our experiments. The calculated optimum design quantum well parameters are shown in Fig. 1. The Figure immediately points to the interesting possibility of reaching short wavelengths, not possible with standard GaAs/$Al_xGa_{1-x}As$ N-QWIPs because of the limited direct bandgap barrier height. Using high Al fractions ($x \sim 1$), cutoff wavelengths approaching ~ 3 μm are expected. Moreover, owing to the broad spectral shape, such a device should cover the wavelength range from 2 to 3 μm.

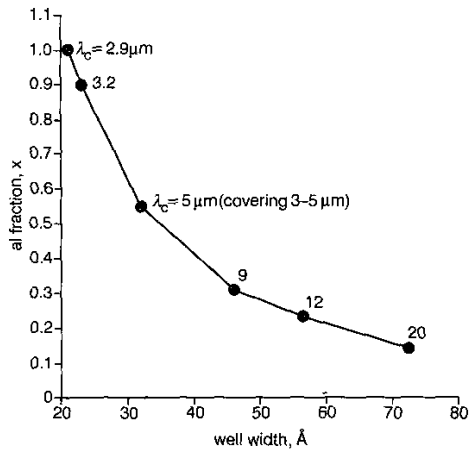

Fig. 1 *Calculated optimum quantum well design parameters*
Point at cutoff wavelength $\lambda_c = 5$ μm has been well studied in our prior work

Table 1: Sample parameters

Sample	Well [nm]	Barrier x	Barrier width [nm]	Doping [cm^{-2}]	Number of wells
A	2.6	0.950	18.6	3×10^{12}	100
B	4.6	0.352	35.6	1.2×10^{12}	100
C	5.7	0.211	45.8	1×10^{12}	75
D	7.2	0.133	73.2	6×10^{11}	50

For all samples, top (0.2 μm) and bottom (0.6 for A and 0.7 μm for the rest) contact layers are doped with Be to 8×10^{18} cm^{-3}. All GaAs well centres are δ-doped with Be with two-dimensional densities listed. Structural parameters have been determined by x-ray measurements.

This Letter presents a study on a set of GaAs/AlGaAs P-QWIPs covering a wide range of wavelengths. Four wafers were grown by molecular beam epitaxy on semi-insulating GaAs substrates. The